RSC Advances

ROYAL SOCIETY OF CHEMISTRY

www.rsc.org/advances

ToC

We fabricated nanoporous microcantilevers using anodic aluminum oxide (AAO) and measured the variations in the resonance frequency and deflection of the cantilever during the adsorption and desorption of water vapor.

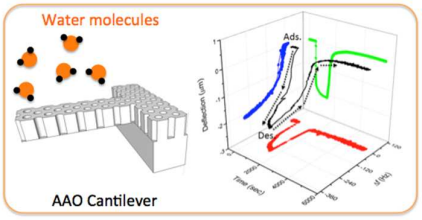

RSC Advances

ARTICLE

Nanomechanical analysis of the adsorption and desorption of water vapor on porous surfaces†

Dongkyu Lee,[a,b] Changyong Yim[a] and Sangmin Jeon[a,*]

Received 00th January 20xx,
Accepted 00th January 20xx

DOI: 10.1039/x0xx00000x

www.rsc.org/

We fabricated nanoporous microcantilevers using anodic aluminum oxide (AAO) and measured the variations in the resonance frequency and deflection of the cantilever during the adsorption and desorption of water vapor. The high surface area and low modulus of the AAO cantilever, due to the presence of the nanopores, permitted the simultaneous measurement of both the changes in mass and surface stress with high sensitivity. The cantilever deflection at the resonance frequency revealed a large deflection change during the early stages of water adsorption and a small deflection change during the later stages. These effects were attributed to the transition from a sub-monolayer water film to a multilayer water film.

Introduction

Water molecules typically adsorb onto a hydrophilic solid surface by forming hydrogen bonds, and the physicochemical properties of the solid are substantially affected by the presence of the adsorbed water.[1] If adsorption occurs on one side of a flat substrate, the adsorbed water affects the surface stress on the substrate and induces substrate bending. The water adsorption-induced surface stress is generally neglected because most substrates, such as a slide glass or a silicon wafer, are too thick to undergo deformation. A sufficiently thin and flexible substrate, however, such as a silicon microcantilever, will bend as water vapor is adsorbed, lending such substrates utility as moisture sensors.[2-5]

Microcantilever sensors are very sensitive to adsorption-induced changes in the sensor surface stress and mass, which may be calculated from measured changes in the deflection and resonance frequency, respectively, obtained from the cantilever. Several studies have examined changes in the surface stress on a microcantilever during the adsorption of a water droplet or water vapor.[2-9] Although the ability to measure orthogonal changes simultaneously increases the versatility of cantilever sensors over competing technologies, such as surface acoustic wave and quartz crystal microbalances,[10-13] previous studies have mainly focused on measuring independent variations in deflections or resonance frequencies.[4,14] It is not straightforward to design cantilever sensors to have high sensitivities in both changes in the mass and stress because stiff (short and thick) cantilevers exhibit a high mass sensitivity whereas flexible (long and thin) cantilevers exhibit a high stress sensitivity.[15]

The contradictory requirements for simultaneous sensitive measurements of changes in the deflection and resonance frequency of a cantilever may be satisfied by fabricating a cantilever with a high surface area and sufficient flexibility. In a previous publication, we described the fabrication of cantilevers with hexagonally ordered nanowells from anodized aluminum oxide (AAO) and used these sensors to investigate the evaporation of a water droplet from a nanowell.[6] The AAO cantilever was found to possess a high surface area and a low modulus due to the presence of nanopores, thereby enabling the AAO cantilever to sensitively measure changes in both the deflection and the resonance frequency at the same time.

In this study, we fabricated nanoporous AAO cantilevers and measured changes in the resonance frequency and deflection of the cantilever during the adsorption and desorption of water vapor. Simultaneous measurements of the orthogonal variations offered two sets of independent measurements as well as a more comprehensive under-standing of the water adsorption process, i.e., the transition from a sub-monolayer water film to a multilayer water film. To the best of our knowledge, this is the first report to investigate changes in the surface stress and mass in situ during the transition between a sub-monolayer water film and a multi-layer water film using a microcantilever sensor.

Experimental

An anodic aluminum oxide (AAO) layer with hexagonally ordered nanopores was fabricated on an aluminum specimen using a two-step anodization process. AAO cantilevers were then fabricated through photolithography and electrochemical etching. Thin films composed of titanium (3 nm) and gold (30 nm) were subsequently coated onto the top sides of the cantilevers to improve the laser reflectivity. A detailed procedure for fabricating AAO cantilevers may be found

[a] Department of Chemical Engineering, Pohang University of Science and Technology (POSTECH), Pohang, Gyeongbuk, Republic of Korea
[b] Current address: Daegu Research Center for Medical Devices, Korea Institute of Machinery and Materials (KIMM), Daegu, Republic of Korea
*Corresponding Author. E-mail: jeons@postech.ac.kr
†Electronic Supplementary Information (ESI) available.
See DOI: 10.1039/x0xx00000x

elsewhere.[6,16] A four-quadrant AFM head with an integrated laser and a position-sensitive detector (Veeco, Santa Barbara, CA) was used to measure the optical deflection of the cantilever. The AAO cantilevers were UV cleaned for 20 min and then immediately mounted inside a quartz flow cell. The resonance frequency of each cantilever was measured using a spectrum analyzer (Stanford Research Systems).

Dry nitrogen (high purity) was passed through a gas bubbler containing deionized water (18.3 MΩ-cm) to generate water vapor. The concentration of water vapor was controlled by adjusting the flow rates of the dry and wet nitrogen streams using mass flow controllers (Brooks Instrument, PA), and the total flow rates were fixed at 100 mL/min. The final concentration of water vapor was calibrated using a commercial moisture sensor (Picotech, Cambridgeshire, U.K.). All experiments were performed at room temperature.

Results and discussion

Figure 1(a) shows scanning electron microscopy (SEM) images of the AAO cantilevers. Figures 1(b) and 1(c) show an enlarged top view image and a cross-sectional image of the cantilever, respectively. The dimensions of the AAO cantilever were 250 μm long, 35 μm wide, and 2 μm thick. The resulting cantilevers featured hexagonally ordered nanopores with diameters and pore-to-pore distances of 50 nm and 100 nm, respectively. The spring constant of the cantilever was measured to be 0.10 N/m using the beam-on-beam method and a silicon cantilever with a known spring constant.[17]

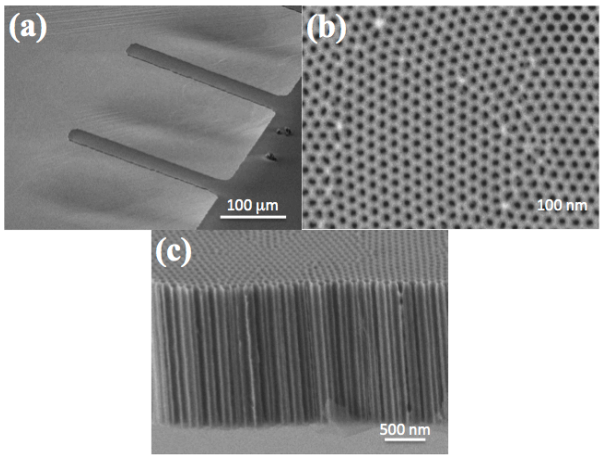

Figure 1. SEM images of the AAO cantilevers at different levels of magnification: (a) top-view image, (b) enlarged SEM image of (a), (c) cross-sectional SEM image of the nanowells.

Figure 2 plots the time dependent changes in the deflection and resonance frequency of the AAO cantilever upon exposure to a relative humidity of 80% (a mixture stream of dry nitrogen and wet nitrogen). The adsorption of water vapor onto the AAO cantilever induced changes in the resonance frequency and deflections in the cantilever. After 25 min of water vapor adsorption (relative humidity of 80 %), the system was rinsed with dry nitrogen (relative humidity of 0 %) to remove adsorbed water. The resonance frequency and deflection of the cantilever returned to the original values, indicating that the adsorption and desorption of water vapor on the AAO cantilever were reversible. The projections of the deflection–frequency–time curve onto each plane correspond to the deflection–time, frequency–time, and deflection–frequency plots, as discussed below.

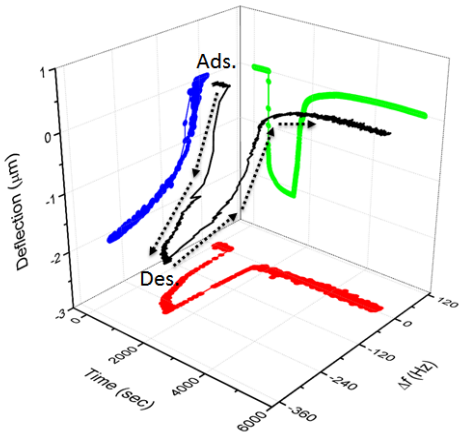

Figure 2. Time-dependent variations in the deflection and resonance frequency of the AAO cantilever upon exposure to a relative humidity of 80%. The projections of the deflection-frequency–time curve (black) onto each plane correspond to the time–deflection (green), time–frequency (red), and frequency–deflection (blue) relationships.

Figure 3 shows the time-dependent variations in the deflection and resonance frequency upon exposure of the AAO cantilever to a relative humidity of 80%. The changes in the deflection (Δ*d*) due to moisture adsorption onto the nanoporous AAO cantilever could be related to the changes in the surface stress (Δ*σ*) using the modified Stoney equation:[18,19]

$$\Delta\sigma = \frac{Et^2(1-P)}{3l^2(1-\nu)}\Delta z \qquad (1)$$

where *E*, *P* and *v* are the Young's modulus, the porosity and the Poisson ratio of the cantilever, respectively. The porosity of the AAO cantilever prepared with hexagonal pores could be calculated using the well-to-well distance (*d*) and the well radius (*r*).[19] The calculated value was 0.23. Because the Young's modulus of the cantilever decreases with the increasing porosity, the deflection sensitivity increases as the porosity increases.

Variations in the resonance frequency of the AAO cantilever were measured simultaneously with the cantilever deflection during the adsorption and desorption of water vapor. Assuming that the spring constant of the cantilever (*k*) was not affected by the moisture adsorption, the variations in the resonance frequency (Δ*f*) could be related to the adsorbed mass of water vapor (Δ*m*),[20]

$$\Delta m = \frac{k}{4\pi^2 n}\left(\frac{1}{f_1^2} - \frac{1}{f_2^2}\right) \quad (2)$$

where f_1 and f_2 are the resonance frequencies of the cantilever before and after adsorption, and n is a geometric factor (0.24), respectively. Although the mass adsorbed onto the cantilever could be calculated using Eq. (2), the estimate was not quite accurate because the nanoporous cantilever surface was not dense or uniform (see the Supplementary Information for the calculation results). It is safe, however, to assume that the frequency change is qualitatively correlated with the mass change. Note that the bare AAO surface could be already hydroxylated during the fabrication processes. The reversible changes in the deflection and resonance frequency of the AAO cantilever during the adsorption and desorption of water vapor indicates that the adsorption of water vapor on the AAO cantilever is physical adsorption.

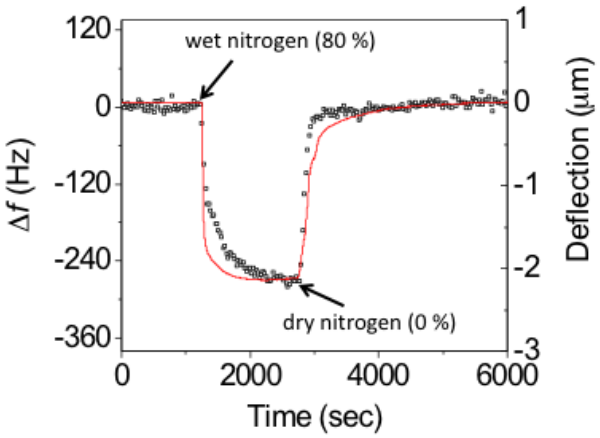

Figure 3. Variations over time in the deflection (red curve) and resonance frequency (open square) of the AAO cantilever upon exposure to a relative humidity of 80%.

Figures 4(a) and 4(b) show the variations in the AAO cantilever deflections as a function of the resonance frequency during adsorption and desorption, respectively. Figure 4(a) shows that the adsorption of water vapor induced relatively large deflections during the earlier stages but relatively small deflections during the later stages for a given change in the resonance frequency (i.e., for a given change in the adsorbed mass). The results obtained from the early and late stages of adsorption were best fit to linear models. The slopes of the adsorption were calculated to be 0.02 and 0.003 μm/Hz for the early and late stage of adsorption, respectively. It is interesting to note that early-stage adsorption induced almost an order of magnitude larger surface stress than late-stage adsorption for a given quantity of adsorbed water. We attributed the change in the slope to a transition from a sub-monolayer water film to a multilayer water film, respectively.[21] The water vapor adsorbed directly onto the cantilever surface until a monolayer had formed, inducing large changes in the surface stress. Further adsorption, however, increased the compressive stress to a lesser degree because the water vapor adsorbed on the wat film rather than onto the cantilever surface. Similar responses were observed during the desorption of water from the nanopores, as shown in Figure 4(b). The early stages of desorption induced relatively small deflections, even though more water molecules desorbed during the early stage than during the late stage.

A control experiment was conducted under a relative humidity of 1% (see the Supporting Information). In contrast with the two characteristic regimes observed at high relative humidities, a single regime was observed at 1% relative humidity, indicating that no transition from a sub-monolayer film to a multilayer film occurred. The slope of the line obtained at 1% relative humidity was 0.014 μm/Hz, nearly equal to the slope observed during the early stage of adsorption at 80% relative humidity, confirming that the adsorption produced a sub-monolayer water film on the AAO cantilever.

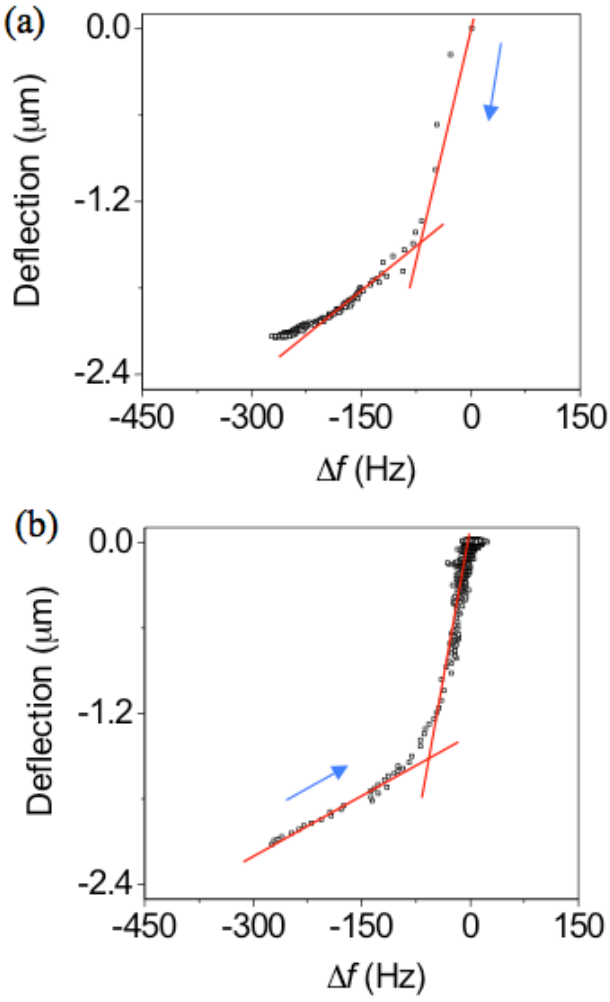

Figure 4. Variations in the deflection as a function of the resonance frequency during (a) the adsorption and (b) the desorption of water molecules. The arrows indicate the directions of adsorption and desorption.

Conclusions

In summary, we fabricated nanoporous AAO cantilevers from anodic aluminum oxide sheets using photolithography and electrochemical etching methods. The presence of nanopores conveyed to the AAO cantilever a high surface area and a low modulus, which enabled us to measure changes in both the mass and the surface stress with high sensitivity upon exposure to moisture. The adsorption of water vapor during the early stages of adsorption induced almost one order of magnitude larger surface stress than the adsorption of water during the later stages of adsorption, for a given mass of adsorbed water. We attributed the differences in the slopes to differences in the adsorption sites on the cantilever. Adsorption proceeded at the cantilever surface during the early stages and at the water film surface during the later stages, which identified the transition from the sub-monolayer water film to the multilayer water film.

Acknowledgements

This research was supported by a Grant No. 14CTAP- C077604-01 funded by Ministry of Land, Infrastructure, and Transport of Korean government.

References

1 M. A. Henderson, *Surf. Sci. Rep.*, 2002, 46, 1–308.
2 C. Y. Lee and G. B. Lee, *J. Micromech. Microeng*., 2003, 13, 620–627.
3 R. H. Ma, C.-Y. Lee, Y. H. Wang and H. J. Chen, *Microsyst Technol,* 2007, 14, 971–977.
4 X. Shi, Q. Chen, J. Fang, K. Varahramyan and H. F. Ji, *Sens. Actuators, B*, 2008, 129, 241–245.
5 A. Boisen, J. Thaysen, H. Jensenius and O. Hansen, *Ultramicroscopy,* 2000, 82, 11–16.
6 M. Lee, D. Lee, N. Jung, M. Yun, C. Yim and S. Jeon, *Appl. Phys. Lett.,* 2011, 98, 013107.
7 E. Bonaccurso and H. J. Butt, *J. Phys. Chem. B*, 2005, 109, 253–263.
8 T. Haschke, E. Bonaccurso, H. J. Butt, D. Lautenschlager, F. Schönfeld and W. Wiechert, *J. Micromech. Microeng.,* 2006, 16, 2273–2280.
9 D. S. Golovko, H. J. R. Butt and E. Bonaccurso, *Langmuir*, 2009, 25, 75–78.
10 T. Nomura, K. Oofuchi, T. Yasuda and S. Furukawa, *IEEE*, 1994, 1, 503–506.
11 T. T. Wu, Y.-Y. Chen and T. H. Chou, *J. Phys. D: Appl. Phys.,* 2008, 41, 085101–4.
12 F. Pascal- Delannoy, B. Sorli and A. Boyer, *Sens. Actuators, A,* 2000, 84, 285–291.
13 X. Wang, B. Ding, J. Yu, M. Wang and F. Pan, *Nanotechnology,* 2009, 21, 055502–7.
14 R. Nuryadi, A. Djajadi, R. Adiel, L. Aprilia and N. Aisah, *Mater. Sci. Forum,* 2013, 737, 176–182.
15 F. Lochon, I. Dufour and D. Rebière, *Sens. Actuators, B*, 2005, 108, 979–985.
16 P.-S Lee, J. Lee, N. Shin, K.-H. Lee, D. Lee, S. Jeon, D. Choi, W. Hwang, and H. Park, *Adv. Mater*., 2008, 20, 1732-1737
17 C. T. Gibson, G. S. Watson and S. Myhra, *Nanotechnology*, 1996, 7, 259–262.
18 P. Kapa, L. Pan, A. Bandhanadham and J. Fang, *Sens. Actuators, B,* 2008.
19 D. Choi, S. Lee, C. Lee, P. Lee, J. Lee, K. Lee, H. Park and W. Hwang, *J. Micromech. Microeng.,* 2007, 17, 501–508.
20 J. W. Yi, W. Y. Shih and W.-H. Shih, *J. Appl. Phys.,* 2002, 91, 1680–1686.
21 H.A. Al-Abadleh and V. H. Grassian, *Langmuir*, 2003, 19,341-347